Electronic Supplementary Material (ESI) for Journal of Materials Chemistry A.

Supporting Information

Reduced Grey Brookite for Noble Metal Free Photocatalytic H_2 Evolution

Ewa Wierzbicka,[1] Marco Altomare,[1]* Mingjian Wu,[2,3,4] Ning Liu,[1] Tadahiro Yokosawa,[2,3,4] Dominik Fehn,[5] Shanshan Qin,[1] Karsten Meyer,[5] Tobias Unruh,[3,4,6] Erdmann Spiecker,[2,3,4] Leonardo Palmisano,[7] Marianna Bellardita,[7] Johannes Will,[2,3,4] Patrik Schmuki[1,8,9]*

1. Department of Materials Science WW4 LKO, Friedrich-Alexander University of Erlangen-Nuremberg (FAU), Martensstrasse 7, 91058 Erlangen, Germany
2. Department of Materials Science Institute for Micro- and Nanostructure Research IMN, Friedrich-Alexander University Erlangen-Nuremberg (FAU), Cauerstrasse 3, 91058 Erlangen, Germany
3. Center for Nanoanalysis and Electron Microscopy (CENEM), Friedrich-Alexander University of Erlangen-Nuremberg (FAU), Cauerstrasse 3, 91058 Erlangen, Germany
4. Interdisciplinary Center for Nanostructured Films (IZNF), Friedrich-Alexander University of Erlangen-Nuremberg (FAU), Cauerstrasse 3, 91058 Erlangen, Germany
5. Department of Chemistry and Pharmacy, Inorganic Chemistry, Friedrich-Alexander University Erlangen-Nürnberg (FAU), Egerlandstrasse 1, 91058 Erlangen, Germany
6. Department of Physics, Institute for Crystallography and Structural Physics, Staudtstrasse 3, 91058 Erlangen, Germany
7. "Schiavello-Grillone Photocatalysis Group", Engineering Department, University of Palermo, Viale delle Scienze, 90128 Palermo, Italy
8. Department of Chemistry, King Abdulaziz University, Jeddah, Saudi Arabia
9. Regional Centre of Advanced Technologies and Materials, Department of Physical Chemistry, Faculty of Science, Palacky University, Slechtitelu 11, 783 71 Olomouc, Czech Republic

* Corresponding Author. E-mail: marco.altomare@fau.de
schmuki@ww.uni-erlangen.de

Experimental Section

In this work, three di□erent TiO_2 polymorphs were used. Commercial anatase and rutile powders samples were purchased from Sigma Aldrich (purity: 99.8%; particle size respectively: anatase 25-35 nm, rutile ~ 60 nm). Brookite samples were prepared via thermohydrolysis of $TiCl_4$ [1,2]. The natural brookite single crystal (5 x 5 mm^2) was purchased by SurfaceNet GmbH (Germany).

Annealing. The hydrogenation (for powders or single crystal) was carried out in pure H_2 at 500°C for durations between 5 minutes and 1 hour, at temperatures in the 300-600°C range, at atmospheric pressure in a flow furnace.

SEM. The morphologies of the as-synthesized samples were characterized by a field emission scanning electron microscope (Hitachi S4800).

TEM. High-resolution transmission electron microscopy (HRTEM) was performed for the powders with a Philips CM30 TEM at an acceleration voltage of 300 KV. The brookite samples were dispersed by sonication in water-methanol mixture (1:1) and drop-casted onto TEM carbon coated copper grids. Geometrical features were measured from TEM images using Image J software.

H_2 evolution. Open circuit photocatalytic H_2 evolution measurements were conducted using 2 mg of powder dispersed into an aqueous methanol solution (50 vol.%) in a quartz tube illuminated with a solar simulator (AM 1.5 G, 100 mW cm^{-2}) for 24 h. A gas chromatograph (GCMS-QO2010SE, SHIMADZU) with TCD detector was used to evaluate the concentration of H_2

generated from the different samples in the head space volume of the sealed quartz tube. For the powder showing the highest photocatalytic activity (H_2 evolution), reproducibility experiments were carried out by repeating different 24h long illumination cycles.

Reflectance. Reflectance spectra for the powders were measured using a UV/Vis spectrophotometer (Lambda 950) in a 800-200 nm wavelength range using an integrating sphere.

EPR. Electron Paramagnetic Resonance (EPR) spectra were recorded on a JEOL continuous wave spectrometer JES-FA200 equipped with an X-band Gunn diode oscillator bridge, a cylindric mode cavity, and a N_2 cryostat. The samples were measured in the solid-state in quartz glass EPR tubes at 95 K with approx. similar loadings. The spectra shown were measured using the following parameters: Temperature 95 K, microwave frequency ν = 8.959 GHz, modulation width 1.0 mT, microwave power 1.0 mW, modulation frequency 100 kHz and a time constant of 0.1 s. Analysis and simulation of the data was done using the software "eview" and "esim" written by E. Bill (MPI for Chemical Energy Conversion, Mülheim an der Ruhr) [3,4].

Photo-electrodes preparation

Electrodes for the photo-electrochemical characterization were fabricated using 0.2 mg of the respective powders in a water/ethanol 50:50 Nafion slurry placed on a carbon electrode. The electrode then was placed in a 3 electrode photo-electrochemical cell as a working electrode. An Ag/AgCl electrode was used as a reference electrode and a Pt plate as a counter electrode. 1 M Na_2SO_4 was used as electrolyte and the applied potential was 0.5 V vs. Ag/AgCl. Illumination was provided by a 150 W Xe arc lamp (LOT-Oriel Instruments) with a Cornerstone motorized 1/8m

monochromator. The monochromized light was focused on a 5×5 mm^2 spot onto the sample surface through a quartz light-pass window in the electrochemical cell. At each wavelength, a photocurrent transient was acquired and the steady state photocurrent was recorded. Photocurrent transients were recorded for 20 s using an electronic shutter system and A/D data acquisition.

Raman spectroscopy. Raman spectra were recorded for Raman shifts between 0 and 1200 cm^{-1} using a confocal Raman spectrometer (LabRAM HR Evolution, Horiba, Dresden, Germany). The 532 nm laser was used as the excitation source. The laser beam was focused on the sample surface with a 10-fold objective. The hole and slit were fully opened at 1200 μm to record the total signal intensity over the sample bulk. The grating was set at 300 gr per mm.

XRD. The crystalline phase composition of the powders was determined using an X-ray diffractometer (X'pert Philips PMD diffractometer) with a Panalytical X'celerator detector and Cu Kα radiation (λ = 1.54056 Å).

Electron Microscopy (single crystal). The FIB lift-out was performed with a Helios NanoLab 660 dual beam system. In order to preserve the native crystal surface, a thick carbon protection layer of a few hundred nanometers were deposited with electron induced deposition, prior to ion-beam processes. The final lamella was targeted at ~80 nm finished with ion-beam showering at 2keV beam energy. In this way, the ion-beam induced sample damage was kept at minimum level. The prepared lamella was characterized with a double Cs-corrected Titan Themis^3 operating at 200 kV. For STEM imaging, we used convergence half-angle of 15.7 mrad, and a camera length of 91.1 mm for simultaneous imaging with multiple detectors: bright-field (BF, with collection

angle range of 0-8 mrad), annular bright-field (ABF, 10-16 mrad), annular dark-field (ADF, 22-50 mrad) and high-angle anuular dark-field (HAADF, 70-300 mrad). SAD patterns were acquired at a camera length of 363 mm, if not noted otherwise, and an SAD aperture of 40 μm and 10 μm in the bulk and at the surface, which translate to selected area diameter of ~200 nm and ~50 nm at the image plane, respectively.

High spatial resolution electron energy-loss spectroscopy (EELS) was acquired using the GIF Quantum ERS, and energy dispersive X-Ray spectroscopy (EDX) was acquired with the Super-X detectors. The datasets were obtained in STEM mode with simultaneous ADF signal also recorded. In the STEM-EELS experiments, the following conditions were applied: probe current 80 – 150 pA, at sampling size (i.e., pixel size) of 0.8 – 1.5 nm/pixel, dwell time 2 – 4 ms, convergence half-angle of 15.7 mrad and EELS collection angle of 44 mrad, spectrometer was set to DualEELS mode, dispersion of the EELS spectrometer 0.25 eV/channel. Under these conditions, good quality EELS spectra suitable for Ti-L23 and O-K fine structure analysis is obtained (i.e., moderately low noise level and final spectra energy resolution at ~1.0 eV measured at the FWHM of the zero-loss peak) while the electron beam induced damage is evaluated to be negligible.

X-ray Diffraction (single crystal). All x-ray patterns were acquired by a Rigaku Smartlab 9 kW, equipped with a Johannson monochromator yielding a divergent copper $K_{\alpha 1}$ beam with a wavelength of 1.54 Å. Whereas for Bragg Brentano measurements the divergence (0.2°) of the beam was exploited, an additional x-ray mirror (CBO-unit) along with in-plane and out-of-plane 0.5° soller collimators were inserted for the GID and XRR measurements. For the GID experiments, the incident angle was 0.27°, thus below the critical angle for Brookite of 0.287°.

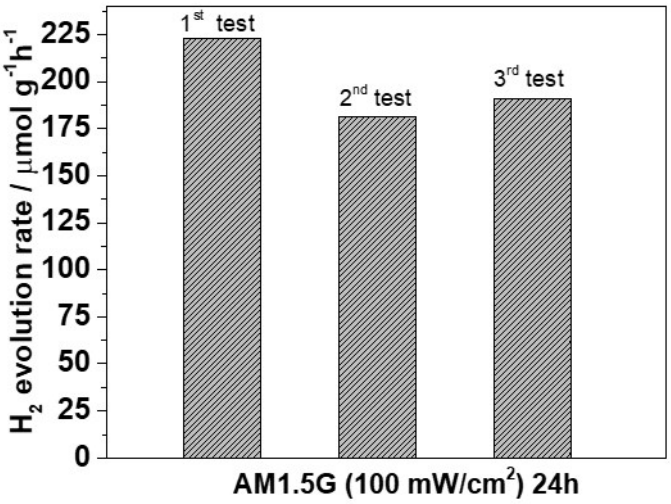

Figure S1. Photocatalytic H_2 evolution of brookite powders hydrogenated under optimized conditions (H_2, 500°C, 10min; sample B-H2-500-10min).

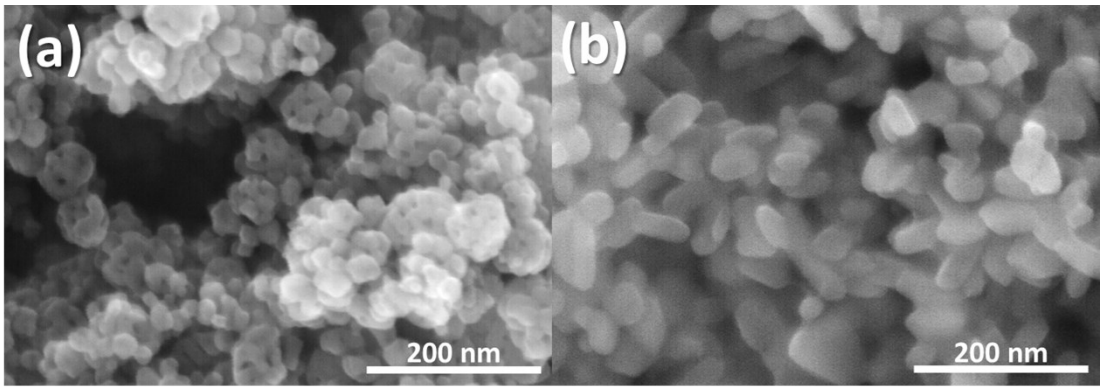

Figure S2. Morphology of (a) anatase, (b) rutile after 10 min annealing at 500 °C in hydrogen.

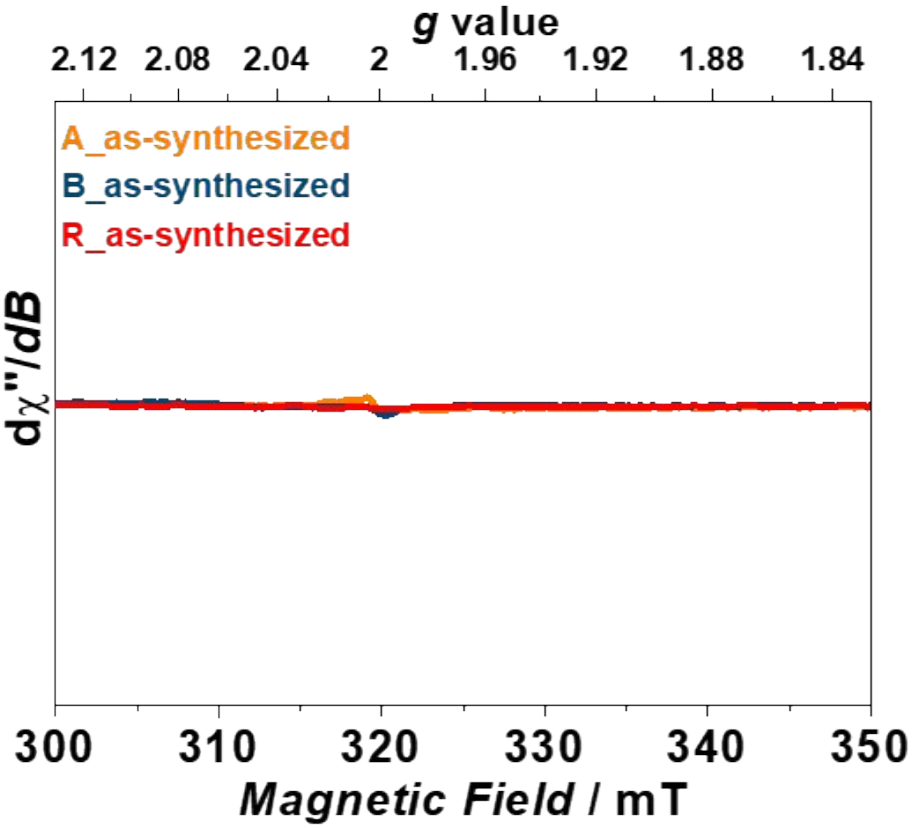

Figure S3. EPR spectra of as-synthesized brookite, rutile and anatase.

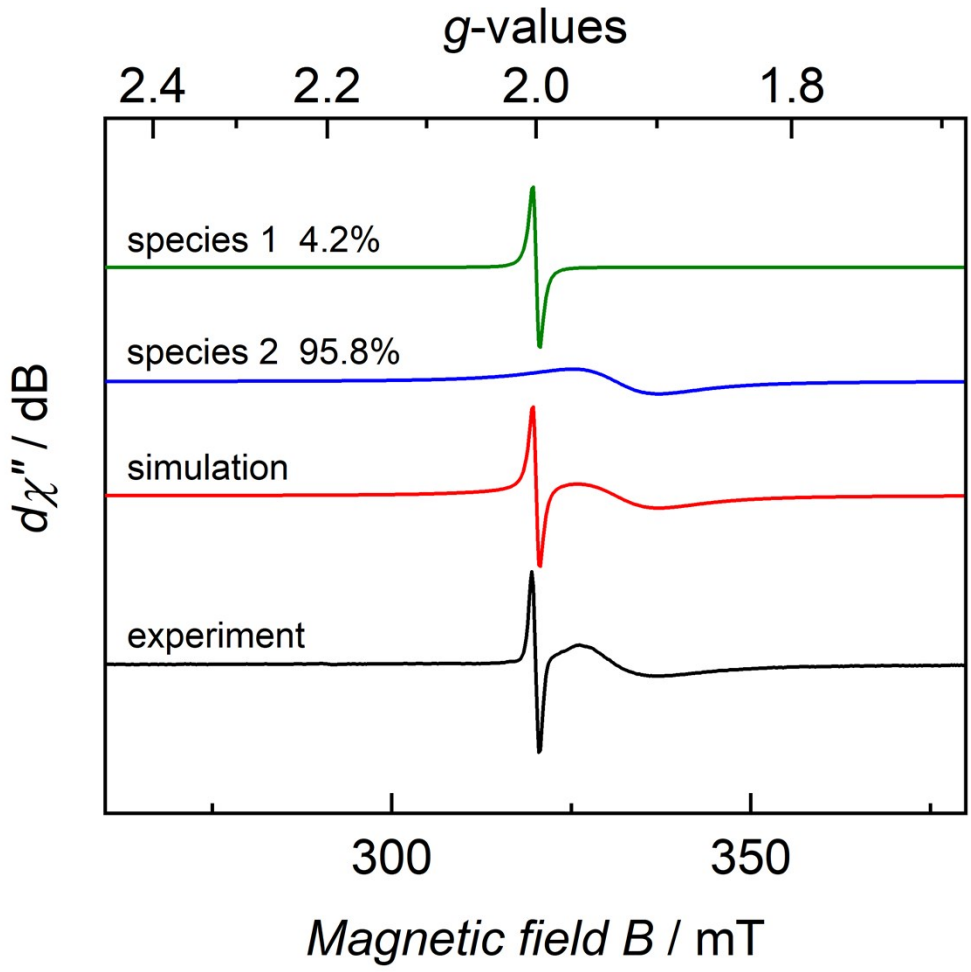

Figure S4. CW X-band EPR spectrum of B-H2-500-10min recorded as a solid at 95 K (black trace), its simulation (red trace), first species (green trace) and second species (blue trace). Experimental conditions: microwave frequency ν = 8.959 GHz, modulation width = 1.0 mT, microwave power = 1.0 mW, modulation frequency = 100 kHz, time constant = 0.1 s. Simulation parameters for species 1: effective spin S = ½, effective g-values giso = 2.00, linewidths Wiso = 1.00 mT, Voigt ratios (Lorentz = 0, Gauss = 1) V = 0.00. Simulation parameters for species 2: effective spin S = ½, effective g-values giso = 1.93, linewidths Wiso = 12.0 mT, Voigt ratios (Lorentz = 0, Gauss = 1) V = 0.00.

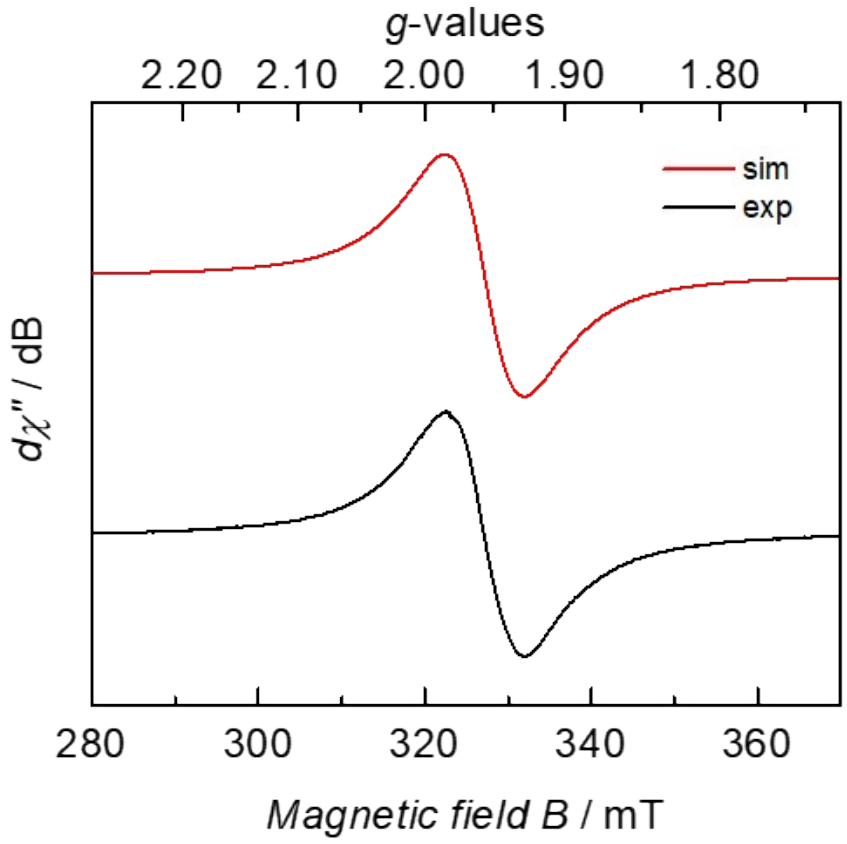

Figure S5. CW X-band EPR spectrum of B-H2-500-1h recorded as a solid at 95 K (black trace), its simulation (red trace). Experimental conditions: microwave frequency ν = 8.959 GHz, modulation width = 0.1 mT, microwave power = 1.0 mW, modulation frequency = 100 kHz, time constant = 0.1 s. Simulation parameters: effective spin S = ½, effective g-values giso = 1.96, linewidths Wiso = 9.69 mT, Voigt ratios (Lorentz = 0, Gauss = 1) V = 0.00.

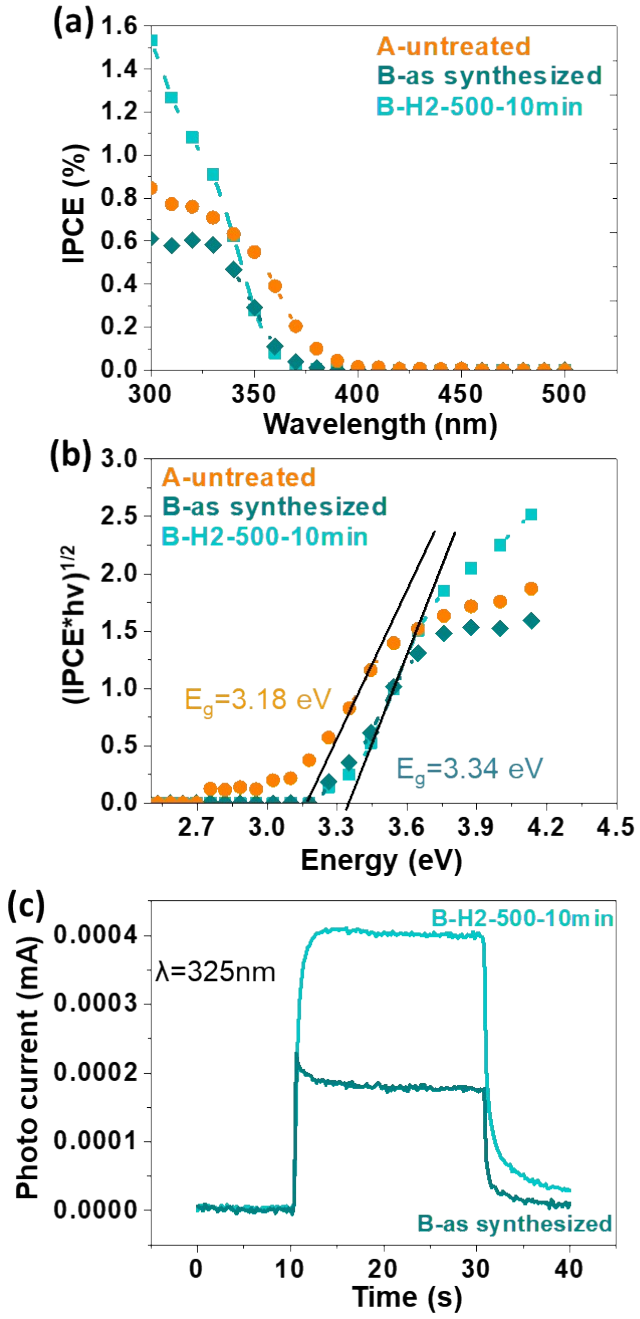

Figure S6. (a) IPCE results of as-received anatase powder, brookite powder before and after 10 min annealing in H_2 at 500°C. (b) Evaluated bandgap from IPCE data. (c) Photo-transients for as-synthesized and grey brookite under light illumination at λ= 325 nm.

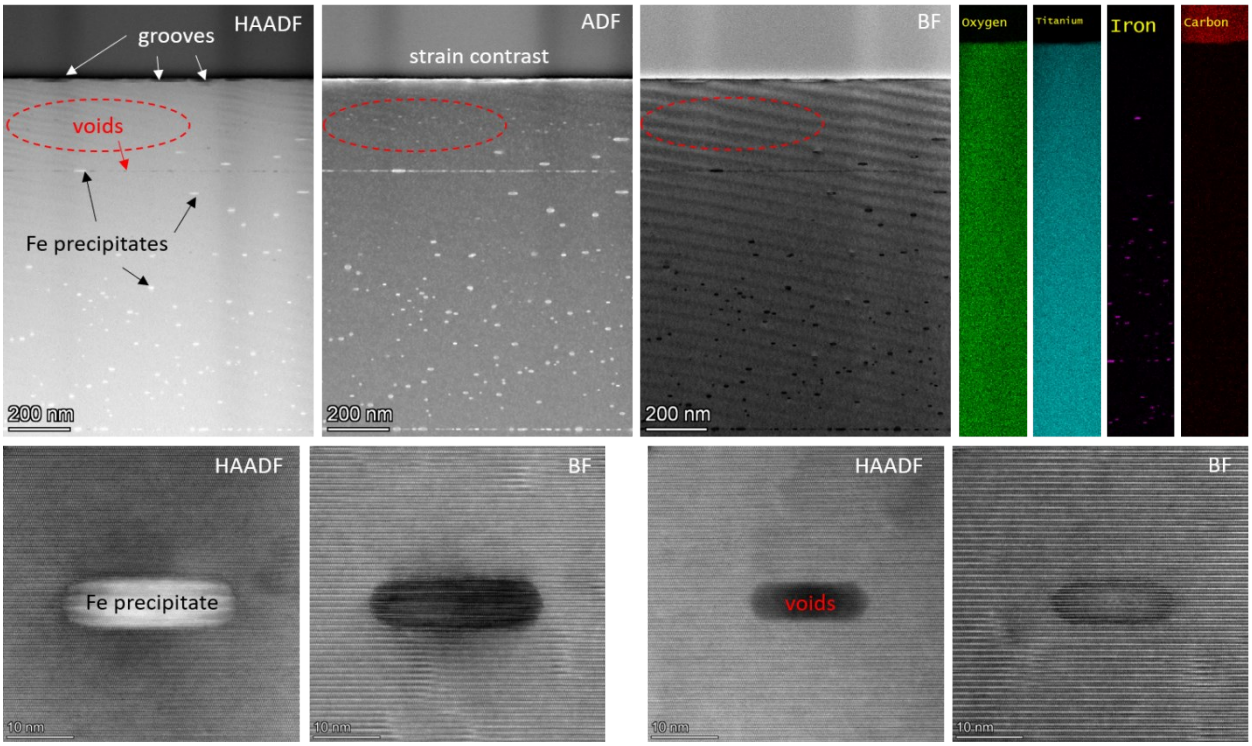

Figure S7. Overview of the hydrogenated brookite sample. Simultaneous HAADF- ADF- and BF-STEM imaging reveals the surface grooves, voids and precipitates in the specimen. EDX-STEM mapping confirm that the precipitates are Fe. The HAADF- and BF- HRSTEM images of the Fe precipitates and voids are also shown. Clear strain contrast at the surface layer can be seen in the ADF-STEM image.

The observed bulk impurities are expected for a natural crystal such as the one used in the present study (macroscopic synthetic brookite single crystals are not available). Two typical types of defects namely precipitates and stacking faults decorated by precipitates are apparent in **Figure S7**. Analytical TEM below as well as x-ray diffraction demonstrates that the precipitates are a coherent α-Fe phase, which further agglomerates during the hydrogenation treatment.

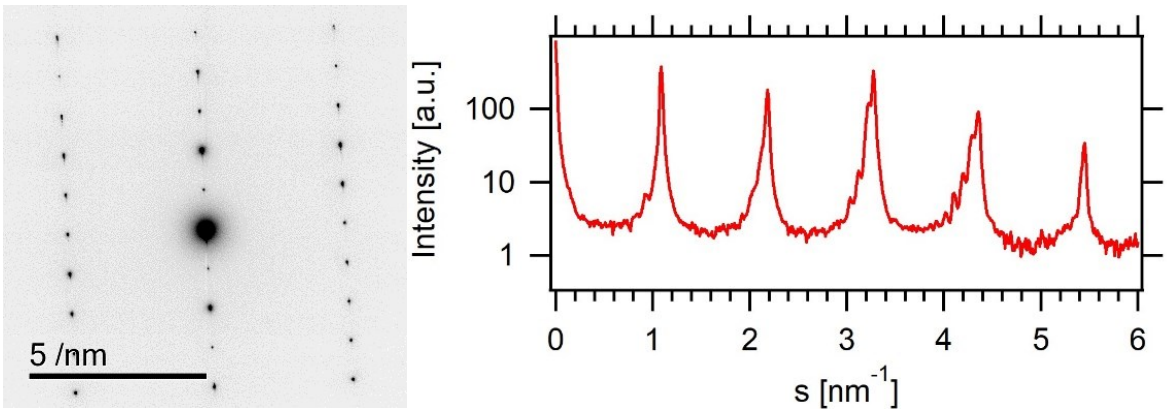

Figure S8. SAD pattern from the surface region taken with a camera length of 722 mm and a SAD aperture of 10 μm (left) along with a line cut along the [00L] direction, exhibiting characteristic Laue fringes.

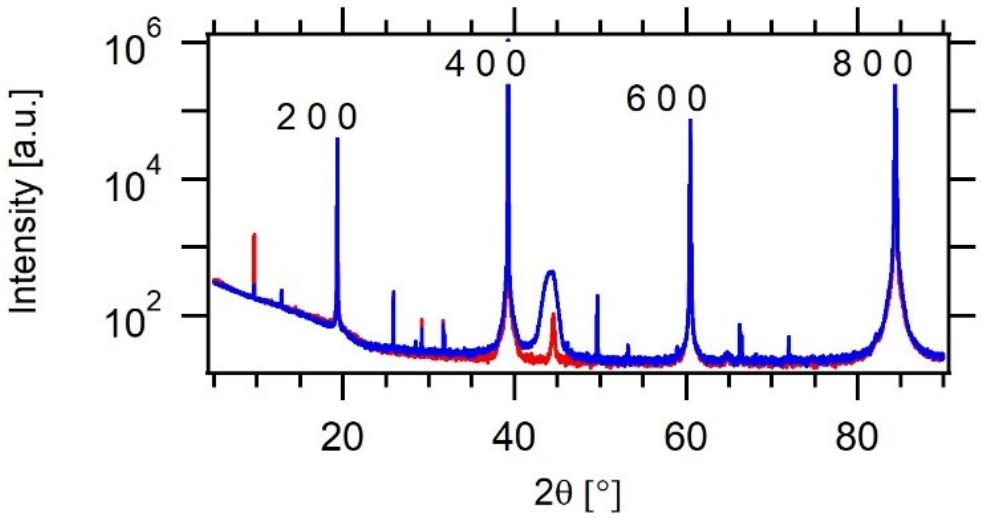

Figure S9. Full θ/2θ scan of the Brookite sample before and after hydrogenation. Brookite peaks are labeled. All other peaks besides the one evolving around 44,7°, which stems from Fe 110, can be attributed to dynamically excited Umweganregungen due to the single crystalline sample in combination with the divergent primary beam. Umweganregungen can be distinguished from primary excited reflections by the peak shape.

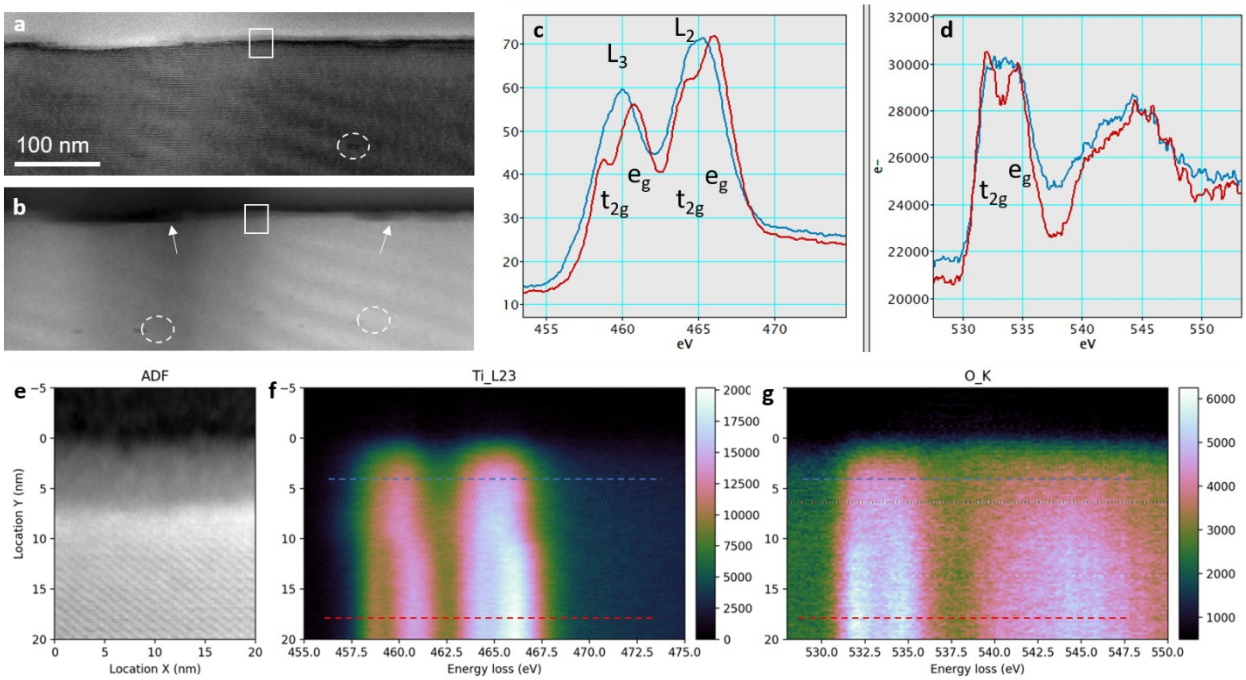

Figure S10. Spatially resolved EELS study of a cross-sectional specimen from the hydrogenated brookite single crystal. (a) STEM-BF and STEM-HAADF (b) overview of a region, where STEM-EELS datasets (white box marked area, results in (c)-(g)) were acquired. The white arrows indicate the surface grooves. Simultaneously acquired STEM-ADF image (e) and EELS spectra of Ti-L23 (f) and O-K (g). The original spectra datacube is rotated and projected, so that the new horizontal axis represents the energy loss and vertical axis correlates to the spatial location from bulk (bottom) to surface (top). Two spectra from the bulk and at the surface is extracted and shown in (c) and (d).

References:

1. Di Paola, A., Cufalo, G., Addamo, M., Bellardita, M., Campostrini, R., Ischia, M., Ceccato, R., and Palmisano, L. (2008) Photocatalytic activity of nanocrystalline TiO_2 (brookite, rutile and brookite-based) powders prepared by thermohydrolysis of $TiCl_4$ in aqueous chloride solutions. Colloids Surfaces A Physicochem. Eng. Asp., **317** (1–3), 366–376.
2. Di Paola, A., Bellardita, M., Ceccato, R., Palmisano, L., and Parrino, F. (2009) Highly active photocatalytic TiO_2 powders obtained by thermohydrolysis of $TiCl_4$ in water. J. Phys. Chem. C, **113** (34), 15166–15174.
3. E. Bill, EPR Program eview, 2019.
4. E. Bill, EPR Program esim, 2019.